Journal of
Marine Science and Engineering

MDPI

Article

Effectiveness of the Speed Reduction Strategy on Exhaust Emissions and Fuel Oil Consumption of a Marine Generator Engine for DC Grid Ships

Van Chien Pham [1], Hanseok Kim [2], Jae-Hyuk Choi [3], Antony J. Nyongesa [1,4], Jongsu Kim [3], Hyeonmin Jeon [3] and Won-Ju Lee [1,3,*]

[1] Interdisciplinary Major of Maritime AI Convergence, Korea Maritime and Ocean University, 727 Taejong-ro, Yeongdo-Gu, Busan 49112, Korea; chien.pham@ut.edu.vn (V.C.P.); tonnyochali@g.kmou.ac.kr (A.J.N.)
[2] Wilhelmsen Ship Management, 1 Sentral, Jalan Rakyat, Kuala Lumpur Sentral, Kuala Lumpur 50470, Malaysia; hanseok.kim@wilhelmsen.com
[3] Division of Marine System Engineering, Korea Maritime and Ocean University, 727 Taejong-ro, Yeongdo-Gu, Busan 49112, Korea; choi_jh@kmou.ac.kr (J.-H.C.); jongskim@kmou.ac.kr (J.K.); jhm861104@kmou.ac.kr (H.J.)
[4] Graduate School, Korea Maritime and Ocean University, 727 Taejong-ro, Yeongdo-Gu, Busan 49112, Korea
* Correspondence: skywonju@kmou.ac.kr; Tel.: +82-51-410-4257

Abstract: Recent developments in power electronics, energy storage systems, and renewable energy; increased market demands for more efficient and cleaner electric power to meet stricter environmental regulations; and development in gigawatt (GW)-class DC (direct current) transmission systems for transmission of greater power over longer distances than similar alternative current (AC) systems, have supported the development of the DC grid, making it a promising solution for both the onshore and offshore industries. This paper presents an experimental study on the effectiveness of an engine speed reduction strategy on exhaust gas emission and fuel consumption when applied to a 4-stroke generator engine equipped with a cam-driven plunger diesel injection system. The experiments were performed on an 8-cylinder V-type 4-stroke generator engine installed in the MASTC laboratory, which is the only demonstration testbed for the ship's electric propulsion system in Korea. Experimental results showed that fuel consumption decreased, but emission mass fraction in exhaust gas increased when maintaining engine power while reducing engine speed. This study has shown economic benefits in reducing fuel consumption, but incurred penalties for the emission performance of 4-stroke generator engines equipped with cam-driven plunger diesel injection systems when applying the engine speed reduction strategy.

Keywords: DC grid system; variable speed generator; engine speed reduction; fuel consumption; exhaust gas emission

check for updates

Citation: Pham, V.C.; Kim, H.; Choi, J.-H.; Nyongesa, A.J.; Kim, J.; Jeon, H.; Lee, W.-J. Effectiveness of the Speed Reduction Strategy on Exhaust Emissions and Fuel Oil Consumption of a Marine Generator Engine for DC Grid Ships. *J. Mar. Sci. Eng.* **2022**, *10*, 979. https://doi.org/10.3390/jmse10070979

Academic Editor: Tie Li

Received: 28 June 2022
Accepted: 15 July 2022
Published: 17 July 2022

Publisher's Note: MDPI stays neutral with regard to jurisdictional claims in published maps and institutional affiliations.

Copyright: © 2022 by the authors. Licensee MDPI, Basel, Switzerland. This article is an open access article distributed under the terms and conditions of the Creative Commons Attribution (CC BY) license (https://creativecommons.org/licenses/by/4.0/).

1. Introduction

In general industry, the direct current (DC) grid system is difficult to transfer electric power over long distances. Meanwhile, the alternating current (AC) grid system can transfer high voltages easily by using transformers, thus it is selected as a standard power system [1].

In the marine industry, most ships have also been using the AC grid system for a long time, except for small boats, due to the advantages of AC grid systems. However, the DC grid system has its own advantages so that it can be applied to some kinds of ships. The preferred ship types for applying a DC grid system might be ferries, cruise ships, small feeder vessels, etc., which employ DC power sources as the primary power source. Moreover, unmanned and autonomous ships have also a high possibility to install full-battery power systems with a DC grid due to low maintenance costs [1]. The other preferred ship types for applying a DC grid system might be offshore service vessels,

multi-purpose support vessels, platform supply vessels, research vessels, anchor handling tug supply vessels, shuttle tankers, drill ships, product carriers, dredgers, drilling rigs, etc., which require variable speed motors with variable frequency drives (VFDs), such as crane motors, pump motors, or dynamic positioning (DP) thrusters [1].

Recently, developments in power electronics, energy storage systems (ESSs), and renewable energy have increased market demands for more efficient and cleaner electric power to meet stricter environmental regulations. The development of gigawatt (GW)-class DC systems (high voltage direct current (HVDC) transmission systems) for transmission of greater power over longer distances than similar AC systems due to them having no reactive power losses, has supported the development of the DC grid and made it a promising solution for both the onshore and offshore industry [1].

In the AC grid system, both frequency and voltage are required to be controlled and monitored in order to maintain power stability. Unlike the AC grid, the DC grid system does not have reactive power interactions. It is, therefore, necessary to control only the voltage of the system. As a result, DC grid systems have the advantage of maintaining power more reliably than AC grid systems. Additionally, in AC grid systems, it is necessary to pay attention to not only voltage and frequency but also to phase angle when synchronizing generators. In contrast, in DC grid systems, only voltage is the important factor and should be taken care of. This means that the synchronization of generators in the DC grid is simpler than in the AC grid.

In view of the power quality in DC grid systems, it is unnecessary to convert an AC to a DC. Therefore, the rectifier part (AC/DC) in the VFDs could be eliminated. This results in reductions in power losses and harmonic distortions during connecting loads. As a result, DC grid systems are well suitable for ships equipped with many VFDs in order to control motors such as propulsion or thruster motors, compressors, pumps, heavy-lifting cranes, etc. [2]. A comparison between the proposed DC grid system and the conventional AC grid system of a pipe-layer ship [3,4] is shown in Figure 1.

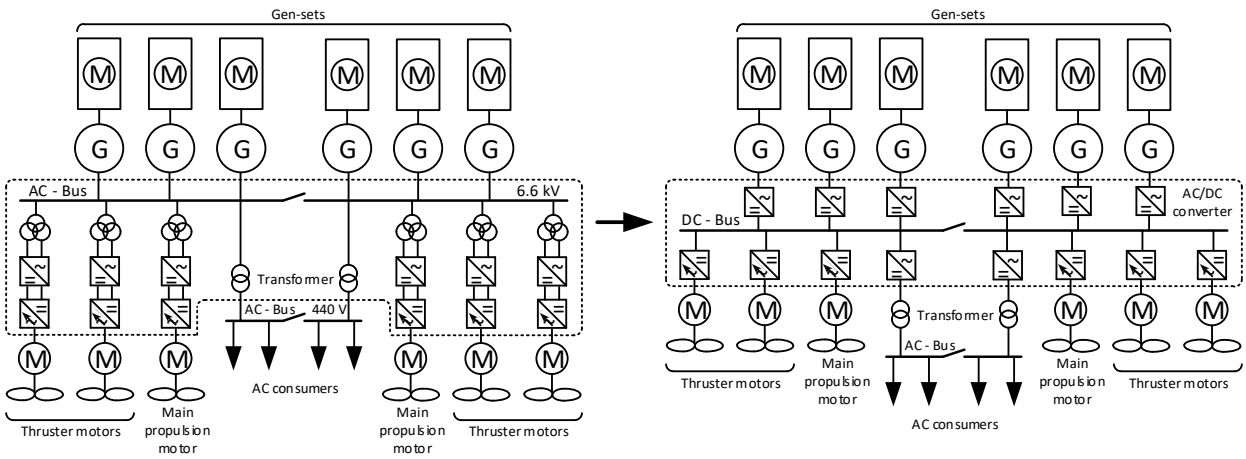

Figure 1. Comparison between the conventional AC grid and proposed DC grid of a pipe-layer ship [3,4].

Also, a DC grid and power-electronics-based power system provide a unique platform for digital solutions onboard a vessel. Equipped with sensors and communication infrastructure, data are transmitted between systems instantly. This gives access to information that enables the bridge to monitor and optimize its performance. Additionally, better connectivity between ship and shore means that performance management is taken to the next level [5].

In view of the economic and environmental aspects, in DC grid systems, gen-sets can operate with variable speeds (frequencies), so they have wider operating windows with high fuel efficiency. It is known that DC grid systems reduce emissions and fuel consumption by up to around 20–40% depending on the ship type and engines [5–8],

reduce greenhouse gas (GHG) emissions due to lower fuel consumption, and reduce particle emissions due to cleaner combustion. In addition, the increase in exhaust gas temperature at lower loads causes the selective catalytic reductions (SCRs) to be fully operational at all load levels, reducing both NOx emissions and urea consumption in the system. The audible noise level can potentially be reduced by more than 5 dB. The maintenance costs can be reduced by up to 30%, and wear and tear on the engine can also be reduced. The combustion process can be cleaner, and thus emits less soot build-up, even when the engine is operated at engine partial loads. An example of a generator engine fuel consumption when running the engine at a fixed speed and at variable speeds is shown in Figure 2 [8].

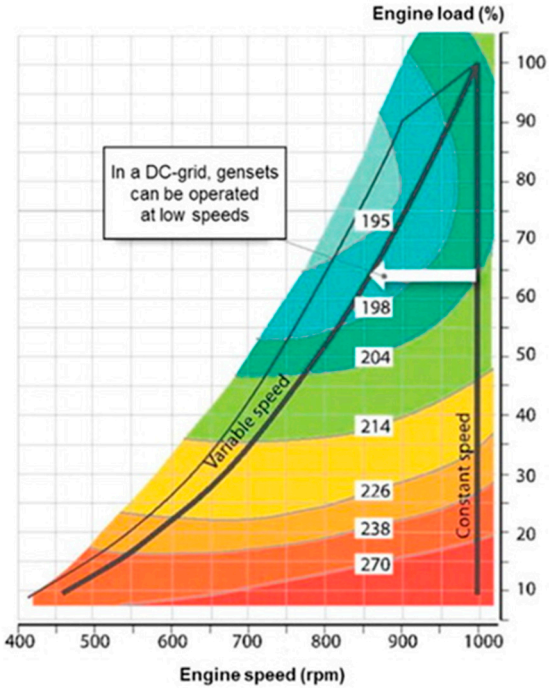

Figure 2. Example of a generator engine fuel consumption graph [8].

According to Figure 2, a big difference in specific fuel oil consumption (SFOC) can be found between the variable speed engine and the constant speed engine in some load cases. For example, at 65% of engine load levels, variable speed engines can have 195~198 g/kWh (light blue colored area) of SFOC, whereas constant speed engines consume 204~214 g/kWh (light green colored area). Similarly, while the SFOC of constant engines is 238~270 g/kWh (orange-colored area) at 25% of generator engine load, the SFOC of variable speed engines would be only 214~226 g/kWh (yellow-colored area). That is, the variable speed generator engine concept in the DC grid system can have better SFOC than constant speed engines in the AC grid system on general load conditions. There are tendencies for bigger differences in SFOC, especially in low load conditions.

In addition, as shown in Figure 2, although the SFOC of both variable and constant speed engines is increased in a low load, the increased SFOC does not have a greater effect on the fuel consumption than when the load is reduced. For instance, in the case of the engine load being reduced from 80% to 40% of the full load in both DC and AC grid systems, the SFOC will only be increased by about 5 to 10%. That is, although the fuel efficiency of the generator engine is decreased in low load, the amount of fuel consumption is eventually decreased. That means that the GHG, especially CO_2 emission, which is directly proportional to the fuel oil consumption, would be reduced as per the load reduction.

Most marine diesel engines have optimal fuel consumption conditions in load levels depending on the tuning condition as per the customer's request. In MAN B&W four-stroke

gen-sets brochures 2021, traditionally gen-sets are optimized at 80–85% MCR (Maximum Continuous Rating) due to limitations in turbocharger matching. However, nowadays new tuning methods optimize the engine performance at approximately 60–65% MCR, as this is often the load range in which gen-sets are operating, but it can also be customized to other specific operating conditions [9]. It means that there is one specific ideal rating for an engine in order to optimize the fuel consumption depending on how the engine is used. In other words, the variable speed engine which can operate at a different speed depending on load conditions can have an unlikely result for the exhaust gas emission.

In another aspect, in ships with many electric motors that require variable speed control, the DC grid system has an advantage in terms of space compared to the AC grid system. This is because in AC grid systems, a phase-shifting transformer, VFD (AC/DC and DC/AC), and LC filter must be installed in front of each motor. Since these devices are installed individually, the AC grid system has disadvantages in terms of space and weight compared to the DC grid system.

As shown in Figure 1, the DC grid system converts AC to DC by using a rectifier at the rear end of the generator. The converted DC is then supplied to various items of equipment on board the ship through the DC bus. In such DC grid systems, the number of AC/DC rectifier installations of VFDs will decrease without the installation of phase-shifting transformers. In the case of electric propulsion ships, space utilization can be maximized in relation to the arrangement of equipment compared to the existing mechanical propulsion method. Conventionally, in the mechanical propulsion method, the main engine-shaft system-propeller connecting system should be located in the center of the ship's engine room. However, in the electric propulsion method, the main electric generators, energy storage systems, power electronic converters, and electric propulsion motors could be installed flexibly. In particular, if the POD (a device which combines both propulsive and steering functions in one device) system is applied, the electric propulsion motor is installed outside the ship's engine room, so it is possible to maximize space utilization.

Additionally, it is very easy to integrate various DC power sources (e.g., lithium-ion batteries, fuel cells, shaft-driven generators, supercapacitors, etc.) into the DC bus. In particular, the ESS could be used independently for various purposes onboard ships. Therefore, it would help to reduce the running time of gen-sets, contributing to reducing maintenance costs and improving energy efficiency.

Lastly, when using DC grid systems, additional generators for harbor use are not necessary, due to variable speed generators having low fuel consumption, even when operating at low and part loads, such as in harbor operations [10].

However, when applying the DC grid system on board ships, it is necessary to pay attention to the issue of protecting electrical equipment connections so that they are always watertight or kept dry, to avoid creating an electrolyte environment for electrolytic reactions that cause DC-current-induced corrosion. DC-current-induced corrosion of steel is of an electrochemical nature. It consists of at least two half-cell reactions: (1) an oxidation reaction at an anode (loss of electron), and (2) a reduction reaction at a cathode (gain of the electron). Coupled cathodic and anodic reactions can cause a small transient in the electric charges. DC-current-induced steel corrosion or oxidization is the result of these electric charges according to Faraday's laws of electrolysis, in which, the amount of substance that reacts or liberates is directly proportional to the number of electric charges passing through it [11]. The condition for an electrolytic reaction to occur is that the anode and cathode must be placed in an electrolyte environment. The presence of chloride in seawater, which can penetrate the connections of electrical equipment on board ships, can be a strong electrolyte environment and cause serious localized corrosion or pitting corrosion.

With regard to engine technology, the internal combustion engine is a thermal engine. It converts the chemical energy of the fuel into mechanical energy on the engine shaft through the combustion of fuels. The thermal efficiency of the engine is, therefore, directly affected by the quality of the combustion process. Among the factors affecting the quality of fuel combustion, the quality of fuel atomization plays an extremely important role. Good

atomization quality increases the quality of mixing of the reactants (fuel and air) in the combustion reaction and, therefore, the quality of combustion, and vice versa [12]. In direct injection diesel engines, the fuel atomization process is mainly controlled by two methods: (1) mechanical control using fuel cams; (2) electronic control. For the mechanical control method, the fuel high-pressure pump is driven and controlled by the fuel cam. The fuel camshaft is driven and synchronized with the engine crankshaft. Therefore, when the engine speed decreases, the rotation speed of the camshaft also decreases accordingly. The decrease in cam rotation speed reduces the pressure rise rate in the high-pressure fuel pump. This reduces the atomization quality of the engine at low speeds. The reduced quality of the fuel atomization reduces the combustion quality, and thus the thermal efficiency of the engine. In contrast to the mechanical control method, the electronic control method can keep the fuel atomization quality at an optimal level and is almost unchanged independent of the engine speed. This is achieved because the electronic control system uses an accumulator (fuel rail) to keep the fuel injection pressure stable and independent of engine speed. The fuel injection pressure is not reduced with the engine speed to help keep the atomization quality stable even when the engine is working at low speeds. The injection timing and duration (fuel amount) are controlled by an electronic Engine Control Unit (ECU) [13–16].

Through the above literature review, the benefits of DC grid systems using variable speed generator engines equipped with electrically controlled fuel injection systems have been demonstrated in many previous studies [1,3,5,7,8]. However, there are very few studies on the effectiveness of a speed reduction strategy when applied to generator engines equipped with cam-driven plunger fuel injection systems in terms of emissions and fuel consumption. The purpose of this experimental study is to identify whether the engine speed reduction strategy is effective on fuel consumption and exhaust gas emission for a 4-stroke generator engine that has a cam-driven plunger diesel injection system which has not been investigated in previous studies. The reason why the effectiveness of the speed reduction strategy needs to be clarified is that the DC grid systems are used with variable speed generator engines, and in variable speed engines, the speed adjusting strategy can reduce fuel consumption and exhaust gas emission in certain conditions.

With this information, the relationship between a fuel consumption, engine speed, engine load, and exhaust gas emission needs to be studied experimentally. In particular, cam-driven fuel injection-system engines are traditionally used for generator engines. All the above are the reason why this research needs to be performed.

2. Experimental Analysis

In order to realize the many economic and environmental benefits of DC grid systems, it was planned to convert the AC grid system of the MASTC laboratory into a DC grid system. In order to ensure the effectiveness of converting the existing AC grid system into a DC grid system in the laboratory, prior to performing the conversation, a number of experiments were conducted aimed at analyzing the effects of the engine speed reduction strategy on exhaust gas emissions and fuel consumption of the engine. The designation of the DC grid system for the laboratory, as well as the experimental setup, procedure, and results, are presented in detail in this section.

2.1. Designing of DC Grid System for the MASTC Laboratory

Figure 3 shows the schematic diagram of the DC grid system, while Figure 4 shows the schematic minimalistic diagram of the DC distribution system designed for the MASTC laboratory. The noise in the power generated by the variable speed engine generator is eliminated by an LC filter. It is converted from AC to DC through the Active Front-End (AFE) rectifier. Table 1 shows the specifications of the AFE rectifier.

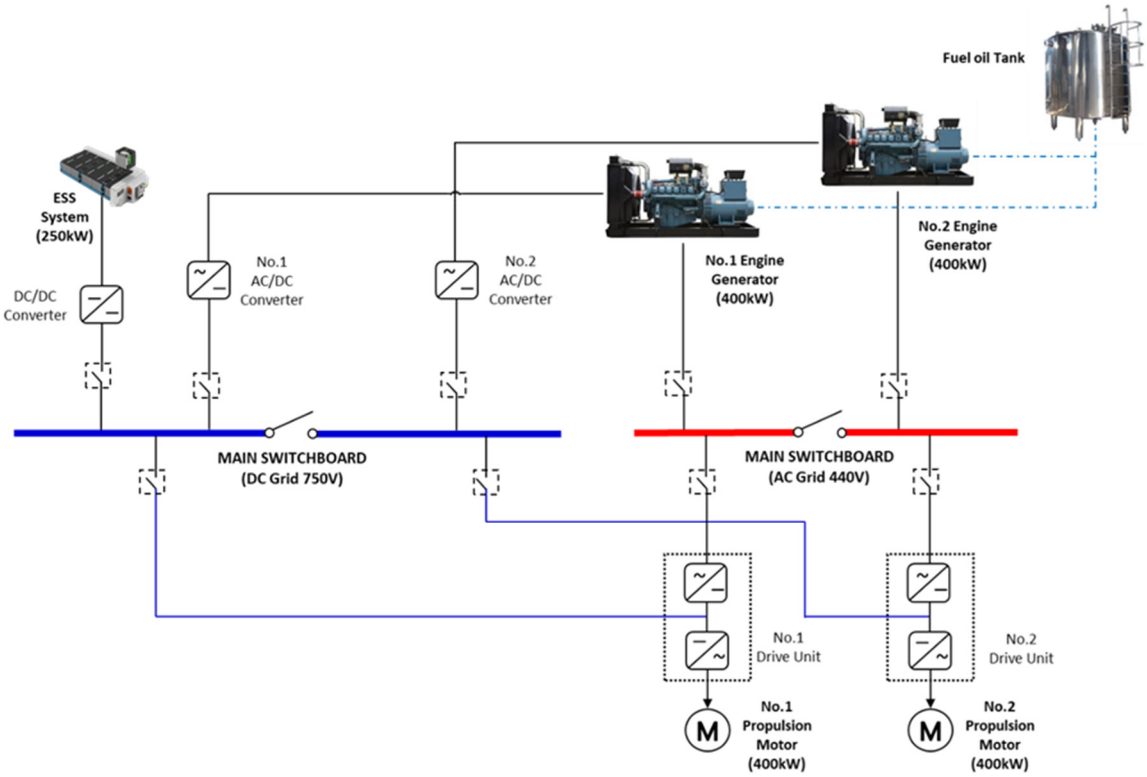

Figure 3. Schematic diagram of the DC grid system designed for the MASTC laboratory.

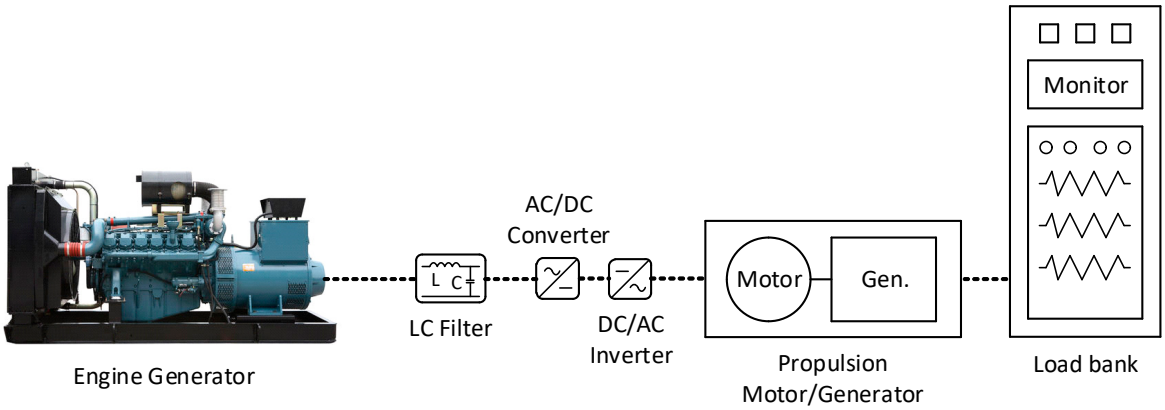

Figure 4. Schematic minimalistic diagram of the DC distribution system designed for the MASTC laboratory.

Table 1. Specifications of the AFE rectifier (AC/DC converter).

Parameters	Value
Capacity	400 kW
Supply voltage	250~480 VAC
Supply frequency	50/60 Hz
Displacement power factor	>0.98
Output voltage	750 VDC
Control voltage	24 VDC
Control current range	0~20 mA

The 750VDC converted through the AFE rectifier is distributed through the DC switchboard. It is controlled by the DC/AC inverter according to the load variation, and the field-oriented control technique is applied to control the propulsion motor. To simulate

the same load environment as a ship, a propulsion motor was installed in connection with a generator and the load bank. Table 2 shows the specifications of the installed DC/AC inverter.

Table 2. Specifications of the DC/AC inverter.

Parameters	Value
Capacity	400 kW
Supply voltage	465~800 VDC
Output voltage	380~500 VAC
Control method	Field Oriented Control
Control voltage	24 VDC
Control current range	0~20 mA

2.2. Experimental Setup and Equipment

In order to analyze the effectiveness of the speed reduction strategy on exhaust gas emission characteristics and fuel oil consumption of the engine, a series of experiments on the Doosan 4-stroke generator engine equipped in the MASTC laboratory were conducted. Figure 5 shows the schematic diagram of the experiments. The engine has V-type 4-stroke 8-cylinders with a cam-driven fuel oil supply system. It is charged with intercooled compressed air supplied by two exhaust gas turbochargers. The specifications of the engine are presented in Table 3.

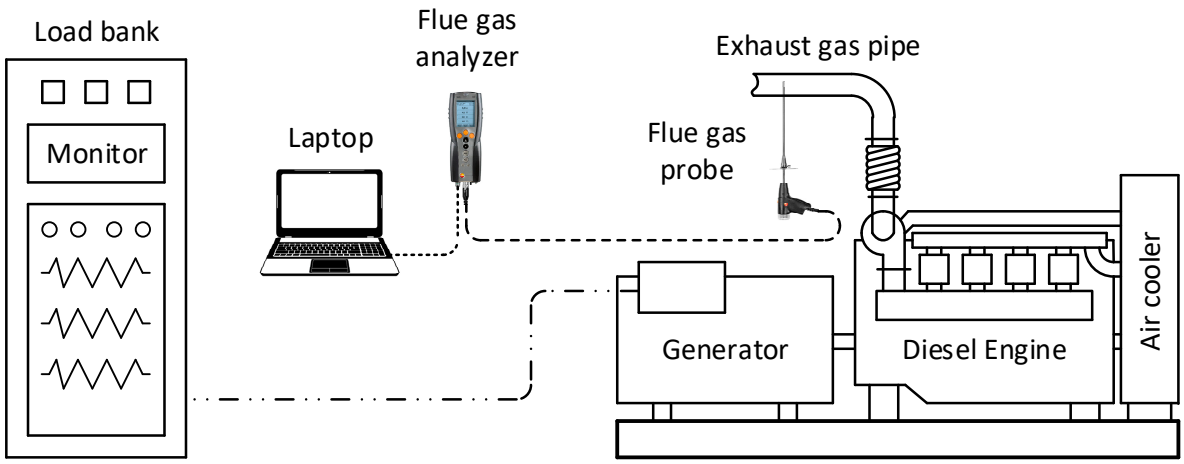

Figure 5. Schematic diagram of the experiment.

Table 3. Specifications of the simulated engine.

Parameters	Value	Unit
Engine type	4-stroke, V-type, 8-cylinder, Turbocharged and Intercooler	
Power × rpm at 100% load	484 kW at 1800 rpm [33.1 kW/L at 1800 rpm]	
BMEP	2.3	MPa
SFOC	129.8	Liters/h
Bore × Stroke	128 × 142	mm
Displacement	14.618	liters
Compression ratio	14.6:1	
Injection nozzle	Multi-hole type	
IVC	36°	ABDC
EVO	62°	ATDC

Loads of the engine are controlled by the load bank. In order to analyze the emissions of the engine, the Testo 350 Maritime v2 flue gas analyzer was used. The Testo 350 Maritime v2 flue gas analyzer has been certified compliant with the requirements specified in Chapter 1, part 7 of "Guidance for the Approval and type Approval of Materials and Equipment for Marine Use" and the relevant Society's Rules. It has also been granted a Type Approval Certificate and found to comply with DNV GL (an international accredited registrar and classification society) rules for the classification-Ships. The analyzer is composed of a measuring instrument and a flue gas modular probe, including sensors for O_2, CO, CO_2, NO, NO_2, and SO_2 detections. The measuring ranges and accuracies of the measuring instrument are presented in Table 4. The flue gas analyzer is connected to computers for monitoring and saving the measured results in real-time during the measurement. The measured results from the flue gas analyzer are then automatically saved to the computer through the Testo 350 Maritime v2 software in terms of Excel files for post-processing.

Table 4. Measuring ranges and accuracies of the measuring instrument.

Measurement Parameter	Measurement Range	Tolerance
−C, Flue gas	−40 to +1000 °C	Max. ± 5 °C
O_2	0 to 25 vol.%	According to MARPOL, Annex VI or NOx Technical Code 2008
CO	0 to 3000 ppm	
NO	0 to 3000 ppm	
NO_2	0 to 500 ppm	
SO_2	100 to 3000 ppm	
CO_2 Infrared Radiation (IR)	0 to 40 vol.%	
P_{abs}	600 to 1150 hPa	±5 hPa at 22 °C ±10 hPa at −5 to +45 °C

In this study, experiments were conducted to evaluate CO, CO_2, and NOx emission concentrations in the engine exhaust gas. Therefore, before conducting the experiments, the CO, CO_2, NO, and NO_2 sensors were tested (calibrated) with the test gas (including CO, CO_2, NO, and NO_2 test gas). The calibration results showed that the deviations between the measured gas and actual gas concentration of the test gases are within the allowable range recommended by the instrument manufacturer. The procedure for performing sensor calibrations of the instrument is presented in Section 6.1.4.4 of reference [17].

In this study, lead-acid batteries play a role as an ESS. They have the function of storing the energy generated by the generator. Therefore, it is also the load of the generator. In the experiments, these batteries serve only as a load changer for the generator, and thus the diesel engine, in case of a need to change the load applied to the engine.

2.3. Experiment Conditions

First of all, although there are two Approval Certificates proving the reliability of the flue gas analyzer, we still wanted to recheck the reliability of the equipment to ensure that the flue gas analyzer would work well for measuring the exhaust gas emissions on the researched engine. Therefore, a number of experiments measuring the exhaust gas emissions of the engine when changing the engine load at the rated speed (1800 rpm) were conducted. In these experiments, we kept the engine running at 1800 rpm, and changed the engine load from 10 to 25, 50, 75, 90, and 100% of the full load. The experiment results showed the same trend in emission formations as mentioned in the literature and previous studies [12,18]. These experimental results confirmed the accuracy of measurements of the flue gas analyzer. The results of these experiments are shown in detail in Section 3.1.

After ensuring the accuracy of the flue gas analyzer, a number of measurement experiments were conducted. In these experiments, the fuel consumption and emissions of the engine when reducing the engine speed while keeping the engine power unchanged

were measured. According to the engine technical report, the engine reaches the best indicated thermal efficiency when running in the load range of 50% and 75% of the full load. Therefore, experiments were conducted at two levels of engine loads, 50% and 75% of the full load. In the case of a 50% load level, the fuel consumption and emissions when operating the engine at 1100 rpm (idle speed), 1300 rpm (medium speed), and 1800 rpm (rated speed) were measured. In the case of a 75% load level, the fuel consumption and emissions when operating the engine at 1300 rpm (low speed), 1500 rpm (medium speed), and 1800 rpm (rated speed) were measured.

For an engine driving a generator, the required power of the engine depends on the electric load level that the generator needs to meet. The electric load of the generator is controlled by the load bank. By varying the electric load level applied to the generator at the load bank, the power that the diesel engine produces to respond to that load will also be changed. To meet the research needs of the laboratory, various electrical loads were designed for this gen-set.

In this study, the standard marine diesel oil (MDO) was used for experiments. Notable differences in pollution emissions for another type of fuel are expected due to the difference in its composition compared to MDO. Therefore, it is important to note that the results presented in this report are for MDO. The main properties of standard MDO are shown in Table 5.

Table 5. Properties of standard MDO [19,20].

Characteristic	Unit	Value	Test Method(s) and References
Kinematic viscosity at 40 °C	mm^2/s	3	ISO 3104
Density at 15 °C	kg/m^3	860	ISO 3675 or ISO 12185
Cetane index	–	40	ISO 4264
Sulfur	mass %	0.05	ISO 8754 or ISO 14596, ASTM D4294
Flash point	°C	62	ISO 2719
Hydrogen sulfide	mg/kg	2	IP 570
Acid number	mg KOH/g	0.5	ASTM D664
Ash	mass %	0.01	ISO 6245
Lower calorific value	MJ/kg	42.7	-

The experiment conditions of measuring fuel consumption and exhaust gas emissions of the engine at different speeds when maintaining the engine load are shown in Table 6.

Table 6. Experiment conditions.

Engine Load [% Full Load]	Engine Speed [rpm]
50	1100
	1300
	1800
75	1300
	1500
	1800

3. Experiment Results

This section presents the experimental results when measuring the exhaust gas emissions and fuel consumption in the cases of operating the engine at (1) the rated speed while reducing engine loads, and (2) keeping the engine load while reducing the engine speed. The results are presented in detail in the following subsections.

3.1. Effects of the Engine Load on Fuel Consumption and Emissions at the Rated Engine Speed

The experiment results when measuring the exhaust gas emissions of the engine in the case of changing the engine load at the rated speed are shown in Figure 6. The results showed that, at the rated engine speed, if the engine load increased, NOx and CO_2 emissions increased while CO emissions decreased. These trends are in line with the literature and previous studies [12,18]. The increasing trend in NOx emission could be explained as the result of increasing the in-cylinder peak temperature when increasing the engine load. It is universally known that NO is the main component and usually accounts for more than 90% of NOx emissions inside the engine cylinder. There are two typical chemical mechanisms for NO formation, including the thermal mechanism (Zeldovich mechanism) and prompt mechanism (Fenimore mechanism) [21]. In order to ensure there is enough air for the fuel to be burned completely, diesel engines are always supplied with an air amount larger than is needed for complete combustion, as in stoichiometric conditions, meaning that the combustion in diesel engines is lean-burn combustion, and the excess air ratio in diesel engines is larger than unity. In such combustion conditions, the NO thermal mechanism plays the most important role and is the biggest contribution to NO formation. With regard to the NO thermal mechanism, the NO formation is greatly influenced by the in-cylinder peak temperature and oxygen concentration within the engine cylinder. NO formation occurs in regions in the cylinder where the local temperature is above 1800 K, and the formation rate increases significantly with the increase of the local in-cylinder temperature [12,21,22]. Therefore, in high engine loads, the in-cylinder peak temperature increases significantly due to the increase in the injected fuel, resulting in an increase in NO emission, and thus NOx emission, as shown in Figure 6.

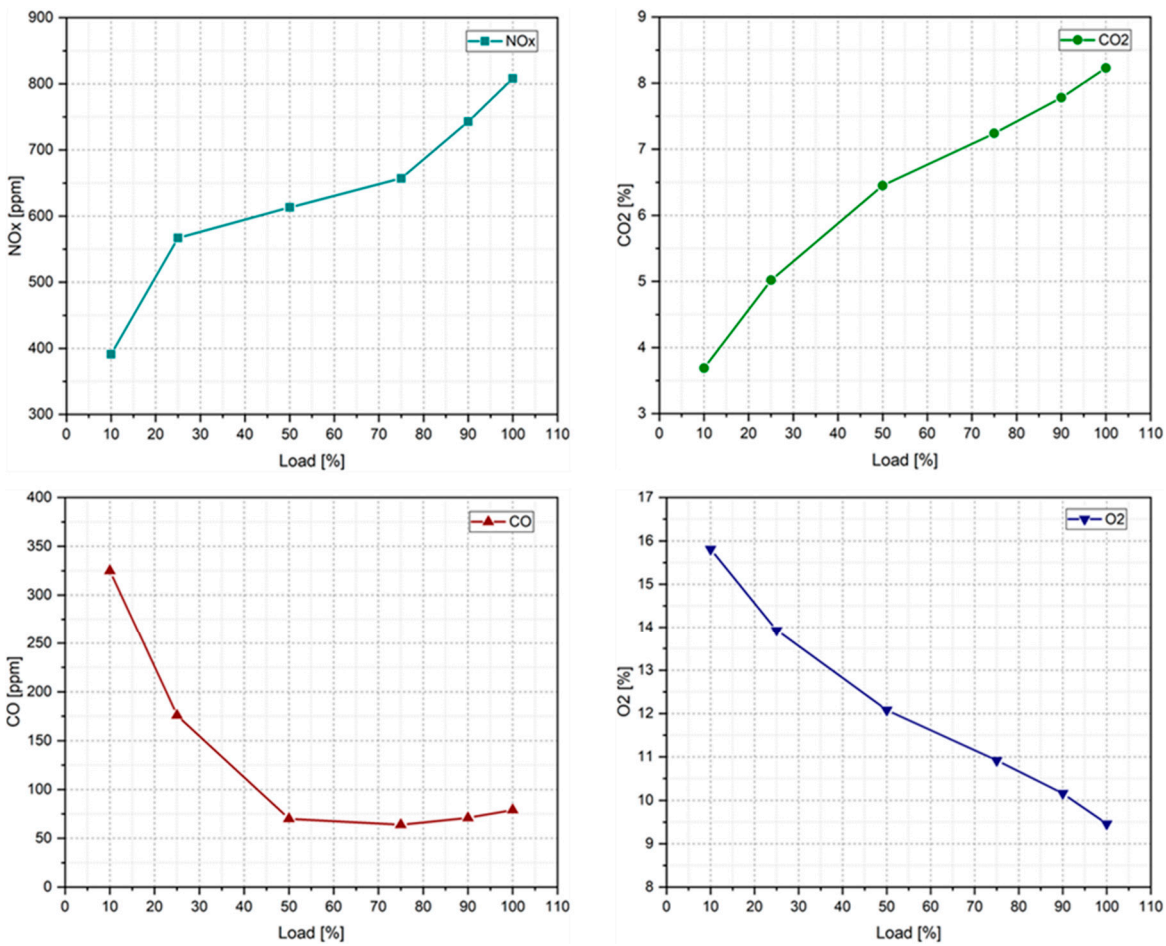

Figure 6. Species concentration analysis when changing the engine load at the rated speed.

With regard to the reasons why there was a reduction trend in CO emission, while CO_2 emission tended to increase when increasing the engine load at the rated speed, as known, CO and CO_2 emissions are the products of fuel combustions, so their formations not only depend on the amount and properties of the injected fuel, but also depend directly on the quality of the combustion process [12]. Carbon dioxide is a product of complete combustions; meanwhile, CO is a product of incomplete combustions of hydrocarbon fuels. Firstly, hydrocarbon fuels will react with O_2 in the charge air to form CO during the combustion process. It is then oxidized to form CO_2 sequentially if the temperature inside the engine cylinder is high enough and there is still enough O_2 in the cylinder for reactions. In other words, CO_2 formation strongly depends on the in-cylinder temperature and the concentration of oxygen in the engine cylinder. When the engine load increases, the operating point of the engine goes to the optimal operating point (in a range of 50–75% of the rated load in the case of this researched engine) and then goes out of the optimal working points. The thermal efficiency is best around the optimal operating point, meaning that combustion reaches complete combustion, and most of the injected fuels will be burned to generate complete combustion products, which is CO_2 emission. Carbon dioxide emission is the product of the CO oxidation process, therefore, an increase in CO_2 formation also means a reduction in CO emissions and O_2 (oxidizer) concentration. At very high engine loads (higher than 75% of full load) which cause the engine working point to exceed its optimal working point, both CO and CO_2 emissions tend to increase due to poorer combustion quality (resulting in an increase in CO emission) and higher injected fuel level (resulting in an increase in CO_2 emission). This is why CO emissions tend to reduce and then increase slightly, while CO_2 emissions tend to increase while increasing the engine load at the rated speed of the engine, as shown in Figure 6. These tendencies have been mentioned in the literature [12] and confirmed by M. A. Ghadikolaei et al. [18]. Through the above analysis, it is reconfirmed that the flue gas analyzer was working well and was suitable to be used for exhaust gas emission measurements in this study.

3.2. Effectiveness of the Engine Speed Reduction Strategy

3.2.1. Effectiveness of the Engine Speed Reduction Strategy on Exhaust Gas Emissions

This section presents the experimental results of exhaust gas emissions and fuel consumption measurements when maintaining the engine load while reducing the engine speed. The experimental results showed that, in both cases of 50% and 75% of the engine full load, the fuel consumption of the engine decreased; however, the mass fraction of emissions in exhaust gas emitted from the engine increased when the engine speed decreased. The mass fractions of NOx, CO_2, and CO emissions of the engine at 50% and 75% load according to the change of the engine speed are shown in Figures 7–9, respectively.

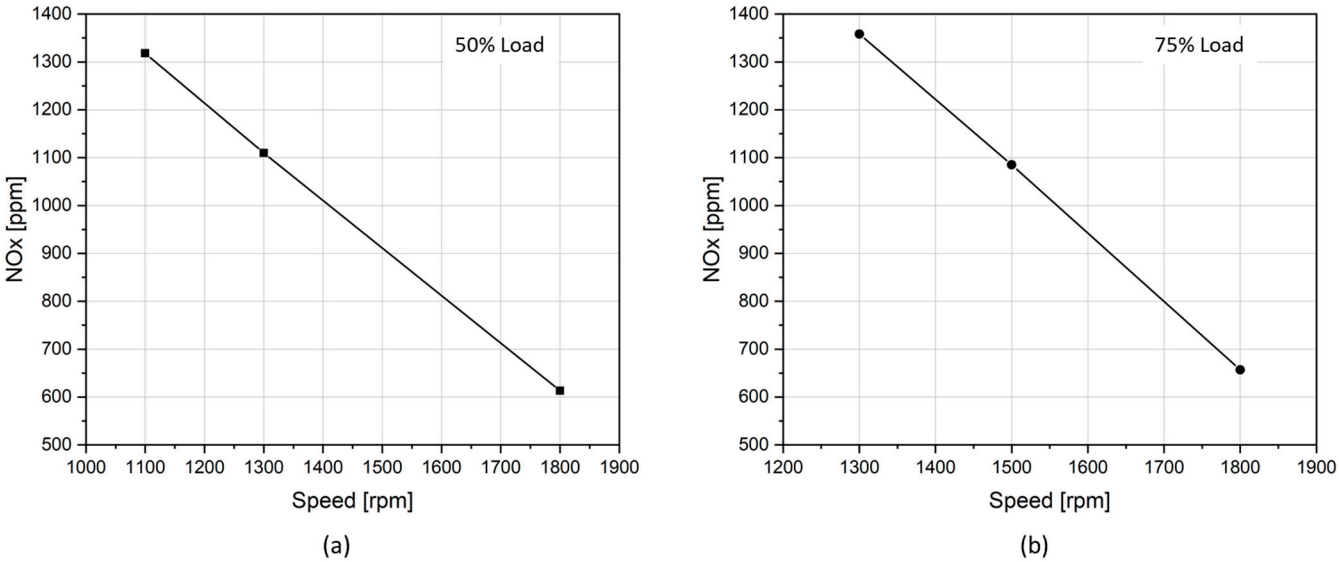

Figure 7. NOx emission according to different engine speeds at (**a**) 50% and (**b**) 75% load.

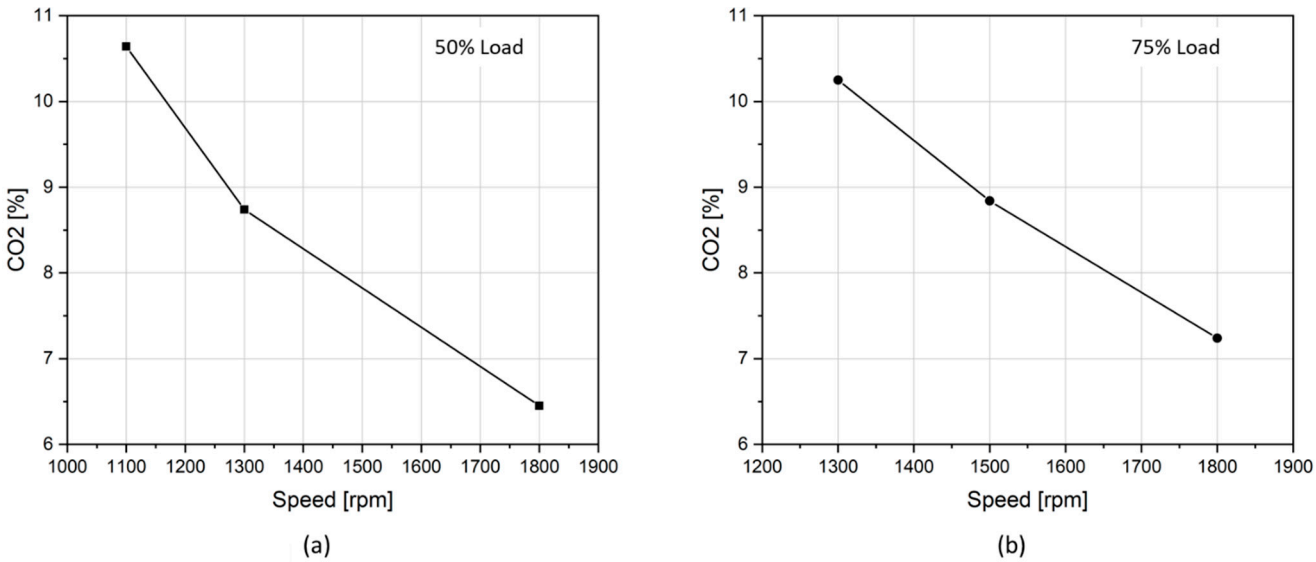

Figure 8. CO_2 emissions according to different engine speeds at (**a**) 50% and (**b**) 75% load.

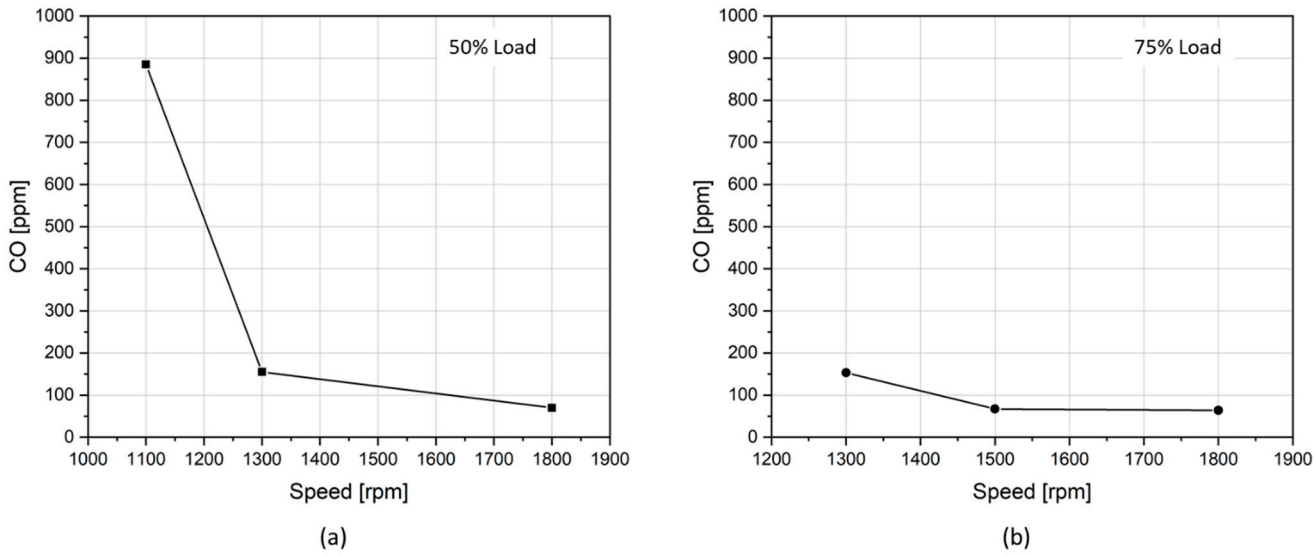

Figure 9. CO emissions according to different engine speeds at (**a**) 50% and (**b**) 75% load.

The increases in emission mass fractions can explained as the result of the increase in the injected fuel per working cycle when reducing the engine speed while maintaining the engine power. The engine power is calculated by Equation (1):

$$P = \frac{10^{-3}}{60} n \times M \tag{1}$$

where P [kW] is the engine power, n [rpm] is the engine speed, and M [Nm] is the engine moment.

According to Equation (1), if we want to reduce the engine speed while keeping the engine power, we must increase the engine moment. Meaning that we must increase the injected fuel per working cycle of the engine. Due to the increase in the one-cycle injected fuel, the emissions emitted from the engine increased as shown in Figures 7–9.

With regard to NOx emission, as mentioned above, the formation of NO emission depends not only on the amount of the injected fuels [12], but also the maximum in-cylinder temperature through the thermal NO mechanism [21]. An increase in the injected fuel at low engine speeds to keep the same engine load resulted in a significant increase in the maximum in-cylinder temperature, causing a significant increase in NOx, as can be seen in Figure 7.

With regard to CO and CO_2 emissions, the formation of CO and CO_2 emissions also not only depend on the amount of the injected fuels, but also strongly depend on the quality of the combustion, that is, the in-cylinder conditions, the air excess ratio, and the fuel atomization quality for combustions [12]. The researched engine was supplied charge air by the two exhaust gas turbochargers and was supplied fuel by a camshaft-driven plunger fuel pump. At low speeds, the efficiency of the exhaust gas turbochargers was reduced, resulting in a reduction in the amount as well as the pressure of the charge air. This resulted in a reduction in both the air excess ratio for combustion and the compression pressure at the end of the compression process. This in-cylinder condition is not good for fuel combustion and negatively affects the combustion quality, leading to increases in exhaust gas emissions.

On the other hand, when the engine is running at low speeds, the moving speed of the piston plunger of the fuel pump is reduced accordingly, resulting in a decrease in the injection pressure. This means that the atomization quality of the fuel injection action is reduced, which then negatively affects the combustion quality, leading to an increase in exhaust gas emissions [23–25]. In addition, since the engine is fueled by a cam-driven fuel injection system, the fuel injection duration is calculated according to the engine crank

angle degrees (CAD) and remains unchanged at all engine speeds. However, if calculated in terms of time (milliseconds), then the fuel injection duration time will increase as the engine speed decreases. In the other words, when the engine runs at a lower speed, fuel is injected into the engine cylinder for a longer time, resulting in a reduction in the injected fuel velocity. This caused a reduction in the mixing quality between the injected fuel droplets and the charge air. Additionally, at low speeds, the swirl of charge air was also decreased, resulting in a further decrease in the mixing quality between the charge air and fuel droplets. All of the above-mentioned factors negatively affected the combustion quality, resulting in increases in CO_2 and CO emissions, particularly at very low speeds, as shown in Figures 8 and 9. This increasing trend in CO emission when decreasing the engine speed has also been presented by Yakup Icingur and Duran Altiparmak [26].

3.2.2. Effectiveness of the Engine Speed Reduction Strategy on Fuel Oil Consumption

Figure 10 shows the brake specific fuel oil consumption (BSFOC) of the engine at 50% and 75% load at different engine speeds. The experimental results showed that, at both engine power of 50% and 75% load levels, the BSFOC was reduced as engine speeds reduced. Specifically, the BSFOC of the engine was reduced from 0.27637 kg/kWh to 0.25254 and 0.24778 kg/kWh when the engine speed was reduced from 1800 rpm to 1300 and 1100 rpm, respectively, in the case of 50% engine load. This means that the BSFOC was reduced by 8.62% and 10.34% when engine speed was reduced from 1800 rpm to 1300 rpm and 1100 rpm, respectively. The BSFOC of the engine was reduced from 0.25994 kg/kWh to 0.24092 and 0.23458 kg/kWh when the engine speed was reduced from 1800 rpm to 1500 and 1300 rpm, respectively, in the case of 75% engine load. This means that the BSFOC was reduced by 7.32% and 9.77% when engine speed was reduced from 1800 rpm to 1500 rpm and 1300 rpm, respectively.

Comparing the BSFOC of the engine at the same engine speed while changing the engine load, the experimental results showed that the BSFOC reduced as engine load increased from 50 to 75% load in both cases of 1300 and 1800 rpm. Specifically, the BSFOC was reduced from 0.25254 kg/kWh to 0.23458 kg/kWh when the engine load increased from 50 to 75% load, equivalent to 7.112%, in the case of 1300 rpm engine speed. The BSFOC was reduced from 0.27637 kg/kWh to 0.25994 kg/kWh when the engine load increased from 50 to 75% load, equivalent to 5.945%, in the case of 1800 rpm engine speed.

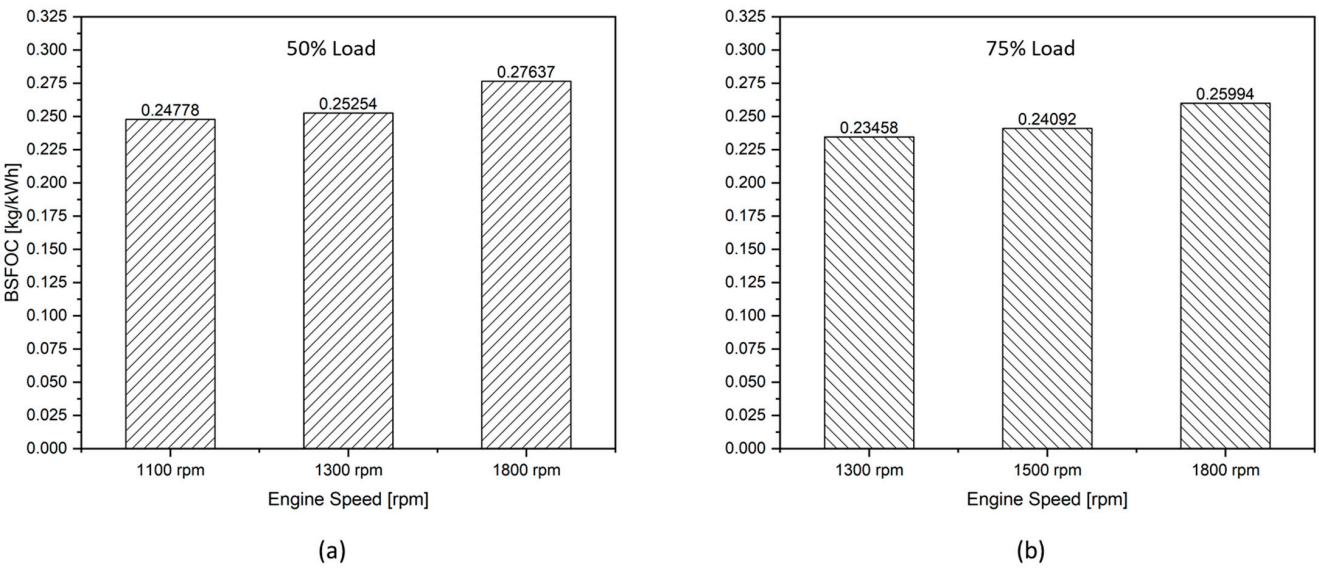

Figure 10. BSFOC of the engine at (**a**) 50% and (**b**) 75% load according to engine speeds.

With regard to the reduction in BSFOC when operating the engine at fixed loads while reducing the engine speed, at fixed engine loads, when the engine speed was reduced,

then even though the injected fuel per working cycle had to be increased as mentioned above, the number of working cycles in one hour decreased accordingly. This resulted in a reduction in specific fuel consumption, i.e., reduction in the amount of fuel used to generate one unit of power in one hour as shown in the experimental result (kg/kWh). This trend is in line with the literature [8] and is also shown in Figure 2. The benefit of the speed reduction (or so-called slow steaming in the maritime sector) strategy on fuel oil consumption reduction has also been reported in other studies [27,28].

In another aspect, reductions in BSFOC when operating the engine at fixed speeds while increasing the engine load are related to the specific fuel oil consumption (SFOC) characteristics of diesel internal combustion engines. As is widely known, when operating engines at fixed speeds, the SFOC of engines will reach the optimal value when engine loads reach from 75–85% of the full load due to the best conditions for the best combustion being achieved in this engine load range [12]. The researched engine in this study is not an exception. That is why the BSFOC of the engine was reduced when the engine load increased from 50% to 75% load in both cases of the engine speed of 1300 and 1800 rpm, as shown in the experimental results.

4. Conclusions and Suggestions

In this work, the effectiveness of the engine speed reduction strategy on the exhaust gas emissions and fuel consumption when applied to a DC grid electric propulsion system using a 4-stroke generator engine equipped with a cam-driven plunger diesel injection system was experimentally investigated. Some major conclusions and discussions drawn from the study are as follows:

1. The fuel consumption was reduced but emission mass fraction in the exhaust gas was increased when the engine load was kept unchanged while the engine speed was reduced.
2. The study showed economic benefits in reducing fuel consumption but incurred penalties for the emission performance of 4-stroke generator engines equipped with a cam-driven plunger diesel injection system when applying the engine speed reduction strategy. In the other words, the engine speed reduction strategy is not suitable for 4-stroke generator engines which use a cam-driven plunger diesel injection system for emission reduction purposes. This is because the combustion quality of engines using a cam-driven fuel injection system is greatly decreased when the engine is running at low speeds, resulting in increases in emissions mass fraction in the exhaust gas.
3. The problems in emission performance of engines might be solved if applying the engine speed reduction strategy on engines equipped with an electronically-controlled fuel injection system, a common rail fuel system, for instance. The highly flexible features of the common rail fuel system help to control fuel injection timing, quantity, and injection pressure independently of engine speed and load. It also offers multiple-injection strategy options for further emission reduction purposes [29]. In such engines, the fuel injection properties can be maintained in the best situation at all engine speeds for the best combustion quality, and thus the best emission performance might be achieved. In this way, both benefits in fuel consumption and exhaust gas emission performance might be achieved at the same time.
4. In practice, it is often difficult to achieve both economic and environmental benefits at the same time. The speed reduction strategy applied to electrically controlled fuel injection engines has been shown to help achieve both of these benefits. However, the present study demonstrated that the engine speed reduction strategy applied to engines with mechanical fuel injection systems only achieves economic benefits without achieving environmental benefits. To achieve both economic and environmental benefits for existing diesel engines equipped with mechanical fuel injection systems, the engine speed reduction strategy is highly recommended in combination with one of two following solutions: (1) converting the existing engine by replacing the

mechanical fuel injection system with a common rail electronic fuel injection system; (2) installing exhaust gas after-treatment devices for the engine (SCR, Scrubber, etc.).

Author Contributions: V.C.P. and H.K. contributed equally to this study. Conceptualization, V.C.P., H.K. and W.-J.L.; methodology, V.C.P. and J.-H.C.; formal analysis, H.K. and J.K.; data curation, H.J. and A.J.N.; writing—original draft preparation, V.C.P. and H.K.; writing—review and editing, V.C.P., H.K. and J.-H.C.; project administration, W.-J.L.; funding acquisition, W.-J.L. All authors have read and agreed to the published version of the manuscript.

Funding: This research was supported by the Autonomous Ship Technology Development Program (K_G012001614001) funded by the Ministry of Trade, Industry and Energy (MOTIE, Korea), and by Korea Institute of Marine Science and Technology Promotion (KIMST) funded by the Ministry of Oceans and Fisheries (20220568).

Institutional Review Board Statement: Not applicable.

Informed Consent Statement: Not applicable.

Data Availability Statement: Not applicable.

Conflicts of Interest: The authors declare no conflict of interest.

Nomenclature

AC	Alternative Current
AFE	Active Front-End
BMEP	Brake Mean Effective Pressure
BSFOC	Brake Specific Fuel Oil Consumption
CO	Carbon monoxide
CO_2	Carbon dioxide
DC	Direct Current
DP	Dynamic Positioning
ESS	Energy Storage System
EVO	Exhaust Valve Opening
GHG	Greenhouse Gas
GW	Giga Watt
HVDC	High Voltage Direct Current
NO	Nitric oxide
NOx	Nitrogen oxides
O_2	Oxygen
IVC	Intake Valve Closing
SCR	Selective Catalytic Reduction
SFOC	Specific Fuel Oil Consumption
SO_2	Sulfur dioxide
rpm	Revolution per minute
VFD	Variable Frequency Device
MARPOL	International Convention for the Prevention of Pollution from Ships

References

1. Kim, K.; Park, K.; Roh, G.; Chun, K. DC-grid system for ships: A study of benefits and technical considerations. *J. Int. Marit. Saf. Environ. Aff. Shipp.* **2018**, *2*, 1–12. [CrossRef]
2. Geertsma, R.; Negenborn, R.; Visser, K.; Hopman, J. Design and control of hybrid power and propulsion systems for smart ships: A review of developments. *Appl. Energy* **2017**, *194*, 30–54. [CrossRef]
3. Hansen, J.F.; Lindtjørn, J.O.; Vanska, K. Onboard DC Grid for enhanced DP operation in ships. In Proceedings of the Dynamic Positioning Conference, Houston, TX, USA, 11–12 October 2011.
4. Kanellos, F.D.; Tsekouras, G.J.; Prousalidis, J. Onboard DC grid employing smart grid technology: Challenges, state of the art and future prospects. *IET Electr. Syst. Transp.* **2015**, *5*, 1–11. [CrossRef]
5. Lindtjørn, J. Onboard DC Grid—A system platform at the heart of Shipping 4.0. pp. 160–167. Available online: https://library.e.abb.com/public/7113040b09fc468d9136944a35e784fa/160-167.pdf?x-sign=MznSn0pXo2QG1pmdoZtO9rq0Yw7TCqITNrxX+zDwnFM1v9P8jlPwUYjziuDGrYK (accessed on 17 May 2022).

6. Settemsdal, S.O.; Haugan, E.; Aagesen, K.; Zahedi, B.; Drilling, S. New enhanced safety power plant solution for DP vessels operated in closed ring configuration. In Proceedings of the Dynamic Positioning Conference, Houston, TX, USA, 14–15 October 2014; pp. 1–21.
7. ABB. *Onboard DC-Grid—The Step Forward in Power Generation and Propulsion*; ABB: Billingstad, Norway, 2011.
8. Wärtsilä. *Machinery—Variable Speed Electric Power Generation*; Wärtsilä: Helsinki, Finland, 2019.
9. Solution, M.E. Marine Engine Program 2021. p. 163. Available online: http://www.stxhi.co.kr/pdf/STXHI%20MAN-ES%20Engine%20Program%202021.pdf (accessed on 10 May 2022).
10. Kokkila, K. Feasibility of Electric Propulsion for Semi-Submersible Heavy Lift Vessels, Marine Heavy Transport & Lift III. *R. Inst. Nav. Archit.* **2012**, *24*, 5–6.
11. Tang, K. Corrosion of steel fibre reinforced concrete (SFRC) subjected to simulated stray direct (DC) interference. *Mater. Today Commun.* **2019**, *20*, 100564. [CrossRef]
12. Heywood, J.B. *Internal Combustion Engine Fundamentals*; McGraw-Hill Education: New York, NY, USA, 2018.
13. Cheon, J.M.; Zin, M.T.; Jung, S. Effect of common-rail pressure and natural gas proportion on performance of dual fuel diesel engine. *J. Adv. Mar. Eng. Technol.* **2020**, *44*, 133–138. [CrossRef]
14. Chen, H.; Su, X.; He, J.; Xie, B. Investigation on combustion and emission characteristics of a common rail diesel engine fueled with diesel/n-pentanol/methanol blends. *Energy* **2019**, *167*, 297–311. [CrossRef]
15. Wang, L.; Li, G.-X.; Xu, C.-L.; Xi, X.; Wu, X.-J.; Sun, S.-P. Effect of characteristic parameters on the magnetic properties of solenoid valve for high-pressure common rail diesel engine. *Energy Convers. Manag.* **2016**, *127*, 656–666. [CrossRef]
16. Fiengo, G.D.G.; Palladino, A.; Giglio, V. *Common Rail System for GDI Engines: Modelling, Identification, and Control*; Springer: Berlin/Heidelberg, Germany, 2013.
17. Testo, I. Testo 350 Maritime v2 Flue Gas Analyser Instruction Manual. 2021. Available online: https://static-int.testo.com/media/30/a7/476842882400/testo-350-maritime-Instruction-manual.pdf (accessed on 19 May 2022).
18. Ghadikolaei, M.A.; Wei, L.; Cheung, C.S.; Yung, K.-F. Effects of engine load and biodiesel content on performance and regulated and unregulated emissions of a diesel engine using contour-plot map. *Sci. Total Environ.* **2019**, *658*, 1117–1130. [CrossRef] [PubMed]
19. Word Fuel Services. *ISO 8217 2017*; Fuel Standard for Marine Distillate Fuels. Word Fuel Services: Miami, FL, USA, 2017. Available online: https://www.wfscorp.com/sites/default/files/ISO-8217-2017-Tables-1-and-2-1-1.pdf (accessed on 17 April 2022).
20. Environment Canada, Emergencies Science and Technology Division. *Marine Diesel Fuel Oil*; Environment Canada, Emergencies Science and Technology Division: Ottawa, ON, Canada, 2015.
21. Wei, L.; Geng, P. A review on natural gas/diesel dual fuel combustion, emissions and performance. *Fuel Process. Technol.* **2016**, *142*, 264–278. [CrossRef]
22. Kuo, K.K. *Principles of Combustion*; Wiley: Hoboken, NJ, USA, 1986.
23. Mohan, B.; Yang, W.; Raman, V.; Sivasankaralingam, V.; Chou, S.K. Optimization of biodiesel fueled engine to meet emission standards through varying nozzle opening pressure and static injection timing. *Appl. Energy* **2014**, *130*, 450–457. [CrossRef]
24. Imtenan, S.; Rahman, S.A.; Masjuki, H.H.; Varman, M.; Kalam, M. Effect of dynamic injection pressure on performance, emission and combustion characteristics of a compression ignition engine. *Renew. Sustain. Energy Rev.* **2015**, *52*, 1205–1211. [CrossRef]
25. Jayakumar, C.; Nargunde, J.; Sinha, A.; Henein, N.A.; Bryzik, W.; Sattler, E. Effect of swirl and injection pressure on performance and emissions of JP-8 fueled high speed single cylinder diesel engine. *J. Eng. Gas Turbines Power* **2012**, *134*, 022802. [CrossRef]
26. İçingür, Y.; Altiparmak, D. Effect of fuel cetane number and injection pressure on a DI Diesel engine performance and emissions. *Energy Convers. Manag.* **2003**, *44*, 389–397. [CrossRef]
27. Lee, C.-Y.; Lee, H.L.; Zhang, J. The impact of slow ocean steaming on delivery reliability and fuel consumption. *Transp. Res. Part E Logist. Transp. Rev.* **2015**, *76*, 176–190. [CrossRef]
28. Zis, T.; North, R.J.; Angeloudis, P.; Ochieng, W.Y.; Bell, M.G. Environmental balance of shipping emissions reduction strategies. *Transp. Res. Rec.* **2015**, *2479*, 25–33. [CrossRef]
29. Gaillard, P.; Hedna, M. *Performance Development of the First European Heavy Duty Diesel Engine Equipped with Full Electronic High Injection Pressure Common Rail System*; SAE Technical Paper; SAE International: Warrendale, PA, USA, 2000; ISSN 0148-7191.